Oceanologia xxx (xxxx) xxx

Available online at www.sciencedirect.com

ScienceDirect

journal homepage: www.journals.elsevier.com/oceanologia

ORIGINAL RESEARCH ARTICLE

General characteristics of tidal currents in the entrance of Khor Abdullah, northwest of Arabian Gulf

Ali Abdulridha Lafta*

Marine Science Center, University of Basrah, Iraq

Received 19 November 2022; accepted 27 March 2023

KEYWORDS
Tidal currents;
Arabian Gulf;
Harmonic analysis;
Residual currents;
Khor Abdullah

Abstract The general characteristics of tidal currents in the entrance of the Khor Abdullah at Iraq marine water, located at the northwest tip of the Arabian Gulf, were studied based on realistic current measurements. The velocity measurements used in this study extended to about one year, which was never previously available in this vital region of the Arabian Gulf. The results illustrated that this area is characterized by strong currents exceeding 1 m/s during both ebb and flood tides, driven by local water level variations. The maximum currents recorded during the study period were 1.65 and 1.36 m/s at the ebb and flood tides, respectively. Additionally, the monthly averages of ebb currents are higher than those of flood currents. The harmonic analysis results revealed that the tidal effect explained approximately 98% of the variation in water currents, with the remaining percentage due to residual currents. Among the 35 tidal components used in harmonic analysis, the M_2 component was the main contributor to tidal currents variation in the area, followed by S_2, K_1, N_2, and O_1. The residual current seems to have a low effect on the currents variations in the area, with maximum values not exceeding 0.0677 and 0.058 m/s during the ebb and flood tides, respectively. The results obtained give a general view of the tidal current behavior and could be beneficial for several aspects of marine and coastal engineering as well as shipping and navigation activities in this region.

1. Introduction

The study of tidal hydrodynamics in coastal water is highly prioritized due to their direct impacts on overall maritime activities and ecosystems stability in these water systems. However, studying tidal hydrodynamics can be useful in understanding the transport and distribution of materials, construction of coastal infrastructure, and shipping processes in harbors and ports. Moreover, it can help determine the appropriate locations for wastewater effluent from industrial

* Corresponding author at: Marine Science Center, University of Basrah, Iraq.
E-mail address: ali.lafta@uobasrah.edu.iq
Peer review under the responsibility of the Institute of Oceanology of the Polish Academy of Sciences.

Production and hosting by Elsevier

https://doi.org/10.1016/j.oceano.2023.03.002

Please cite this article as: A.A. Lafta, General Characteristics of Tidal Currents in the Entrance of Khor Abdullah, Northwest of Arabian Gulf, Oceanologia, https://doi.org/10.1016/j.oceano.2023.03.002

and domestic activities. Among the main oceanic currents, tidal currents play a fundamental role in physical processes in coastal regions. Tidal currents are generated and coincide with the rising and falling of the tide; the vertical motion of water causes the water to move horizontally, creating currents (Boon, 2013). Generally, tidal currents are responsible for water exchange processes between the coastal and open sea, consequently, they are the most essential mechanism responsible for the transport of material from or to the coastal systems (Kowalik et al., 2015; Sterl et al., 2020). However, tidal currents can break up pollutants or carry them farther toward the open sea. Moreover, tidal currents have the most significant effect on sediment transport in the coastal regions and, thus, on morphological changes by inducing erosion or sedimentation processes in these areas (Truong et al., 2021). Furthermore, understanding the tidal currents patterns could enhance navigation safety, particularly in the shallow coastal regions at the entrance of bays or estuarine systems.

Traditionally, there are two direct ways to measure tidal currents, the Lagrangian and the Eulerian methods (Poulain and Centurioni, 2015). Tidal currents measurements by the Lagrangian method are conducted simply by adding something to the water and following it as it moves. Meanwhile, the Eulerian approach involves placing an instrument in a fixed position and measuring how fast the water flow at that location. The most valuable data on tidal currents, particularly for long periods of observations, could be obtained by installing special instruments anchored to the seafloor (moorings) or mounted on buoys and platforms. Nowadays, the ADCP (acoustic Doppler current profiler) technique is widely used around the world to measure the flow velocity in both coastal and open seas due to their flexibility and accuracy in conducting such measurements (Bi et al., 2019; Hoitink et al., 2009; Shin et al., 2022).

Iraq marine water, located at the northwest tip of the Arabian Gulf, is the most estuarine part of the gulf, consisting of the Shatt al-Arab estuary and several open lagoons, such as Khor Al-Kafka, Khor Al-Amaya, and Khor Abdullah (Al-Mahdi et al., 2009). Iraq's marine water is critical to the country because it is the only way to reach the open sea (Lafta et al., 2020). The Arabian Gulf is the world's most important oil transport waterway, and it receives a great deal of attention from researchers in various scientific fields, particularly oceanographic studies (Alosairi et al., 2011; Alothman and Ayhan, 2010; Kämpf and Sadrinasab, 2006; Lafta, 2021; Madah and Sameer, 2022; Ranjbar et al., 2020; Reynolds, 1993; Sadrinasab and Kämpf, 2004; Siddig et al., 2019). However, physical oceanographic studies at the gulf's northwestern tip, particularly those based on field measurements, remain incomplete and require further investigation. However, Arabian Gulf is familiar with strong tidal currents, which coincide with a high tidal range that exceeds 1 m in all gulf regions (Alosairi et al., 2011; Reynolds, 1993). Najafi (1997) predicted that the tidal currents can reach 0.9 m/s in the gulf head and range between 0.3 and 0.6 m/s elsewhere. However, the measurements of tidal currents in Iraq marine water are very scarce, and if available, they are limited to short periods. Al-Mahdi et al. (2009) conducted one of the first studies that highlighted the physical characteristics of Iraq's marine water. They indicated that the tidal currents in the entrance of Khor Abdullah are strong and reach speeds of the order of 1—2 m/s. Al-Mahdi and Mahmood (2010) studied the features of tidal currents at the entrance of Khor Abdullah and indicated that the mean flood currents are higher than the mean ebb currents. Moreover, they showed a reduction in the speed of currents with the depth. Moreover, Al-Hasem (2018) was the first to study the tidal currents characteristics based on a continuous measurement of flow velocities near our study area. However, he studied the behavior of tidal currents using hourly records of flow velocities for about 54 days near the entrance of Khor Abdullah on the Kuwait coast. He showed that the maximum flood and ebb velocities reach 1.07 and 1.08 m/s, respectively. This study aims to examine the general characteristics of the tidal currents at the entrance of Khor Abdullah in Iraq marine water located at the northwestern tip of the Arabian Gulf based on a relatively long record of the velocity of the currents.

2. Material and methods

2.1. Study area

Iraq marine water is located at the northwest tip of the Arabian Gulf. The area is known as a waterway of oil transportation and oil industries for mega oil fields in southern Iraq, as well as its economic importance for the country due to the shipping processes by several commercial ports. Figure 1 shows the location of the study area and the ADCP and tide gauge sites. However, the study area is located in the most shallow water region of the gulf, with depths ranging from 10 to 20 m.

The tidal regime in the region is mixed, primarily semidiurnal, with the essential tidal constituents being the semidiurnal M_2 and S_2 and diurnal K_1 and O_1 (Lafta et al., 2020; Lafta, 2022).

The climate of this region is characterized by an arid desert climate with two distinct seasons: a hot and long summer of about 230 days and cold and rainy winter (Zakaria et al., 2013). Rainfall occurs during the winter months, and its average is generally low, with a negligible contribution to the water budget in Arabian Gulf (Reynolds, 1993). The prevailing wind regime in the northwest of the Arabian Gulf is the northwest wind, locally known as the Shamal wind. This wind blows on the area during most months of the year with notable seasonal variations. The second important wind regime in the region is the southeast wind; its period ranges from hours to several days (Reynolds, 1993). The averages of wind speed are higher in summer than those in winter. The peak wind speeds are generally due to the northwest wind and the maximum wind speed can exceed 20 m/s. On the other hand, although the southeast wind speed is generally lower than that of the northwest wind, the highest wave heights in the studied area were recorded during the southeast wind, which is mainly attributed to a large fetch available for the southeast wind relative to a limited fetch available to the northwest wind (Lafta and Al-Fartusi, 2022). The wind waves are dominant in the area with negligible contribution due to swell waves. The highest observed significant and maximum wave heights reach 0.78 and 1.95 m, respectively (Lafta and Al-Fartusi, 2022).

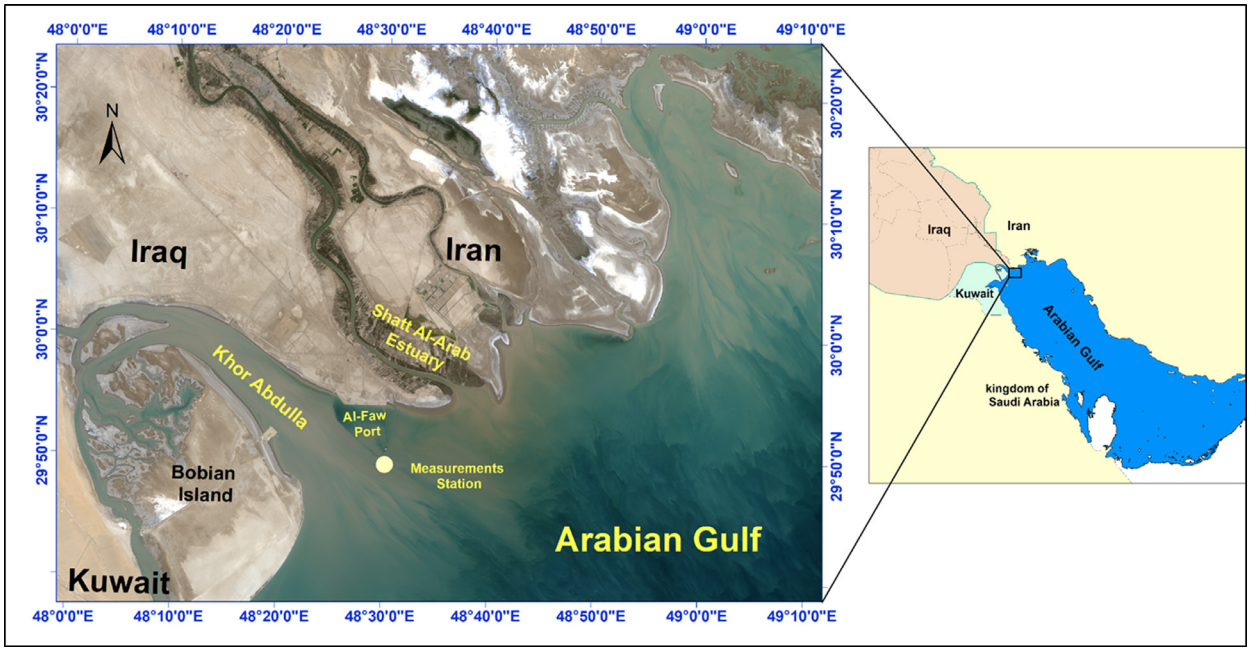

Figure 1 Location map of the study area showing the measurements station (Lafta, 2021).

2.2. Harmonic analysis of currents

The harmonic tidal current analysis is widely used to obtain the amplitudes and phase lags for each tidal frequency (Chen et al., 2021; Jin et al., 2018; Khedr et al., 2018). The traditional harmonic tidal model involving tidal and nontidal energies can be expressed as follows:

$$h(x,t) = h_0 + \sum_{j=1}^{m} f_j H_j \cos\left(\omega_j t + u_j - k_j^*\right) + R, \quad (1)$$

where t is time in hours, h(x,t) is the water level or water current at time t, f_j is the lunar node factor for constituent, H_j is the amplitude for constituent, h_0 is the mean water level or water current in that location, u_j is the nodal phase for constituent, k_j^* is the phase of constituent, ω_j is the frequency of constituent, m is the number of constituents, and R is the nontidal residual. For purely solar constituents, $f_j = 1$ and $u_j = 0$. The residual currents, which are generated by forces other than astronomical tidal forces, play an important role in coastal hydrodynamics (Antoranz et al., 2001). Residual currents control the transport of sediment and consequently largely contribute to long-term morphological changes in coastal regions. Additionally, residual currents control the transport and fate of pollution, which has a considerable effect on the environmental stability of coastal water.

The MATLAB World tide and World Currents, a package for tide and tidal current analysis was used in this study (Boon, 2013). The World Currents package analyzes water currents based on the assumption that horizontal currents can be converted into two components, U and V. However, in the entrances of estuaries and lagoons, the currents display reverse directions associated with flood and ebb phases of the tidal cycle. Hence, by separating currents into two components, obviously, there will be the principal axis U and secondary axes V. The idea proposed by World Currents package is that if there is a distinguished direction of flood and ebb currents, then the orthogonal axes (U, V) can rotate to correspond to the water current directions while keeping the dots (data of water velocities) fixed. The principal and secondary axes resulting from the rotation of U and V are denoted as U_p and V_p. The total variance, the combined variance for U_p and V_p, will be the same as that for U and V. However, the principle axis U_p will have the greatest fraction possible of the total variance and V_p will have the least. If the U_p fraction is high enough, we may choose it and ignore V_p altogether, reducing the current's dimensionality from two to one (Boon, 2013). The U_p current component is one needed for the tidal current analysis, and we can now analyze a current curve plotted as a continuous function of time.

2.3. Data source

Generally, water currents measurements in Iraq marine water are very scarce, and when available, they are generally limited for a short period that does not exceed one tidal cycle. In the past decade, Daewoo Engineering and Construction Co., Ltd., which constructed the western breakwater of the Grand Faw Port, installed a hydrographic station at the entrance of Khor Abdullah, about 700 m far from the breakwater at 29°50′1.8″N, 48°28′43.8″ E (Figure 1). The water depth at this location reaches 10 m. Several oceanographic and meteorological elements are recorded continuously by this platform. These data are managed under the responsibility of the General Acoustics company, Germany (https://www.generalacoustics.com/).

The continuous records of the water currents for January 2018 to November 2018 and the water level of 2018 were acquired by the General Company for Ports of Iraq. The water level measurements are carried out by installing an acoustic tide gauge above the platform at a height of 4.98 m relative

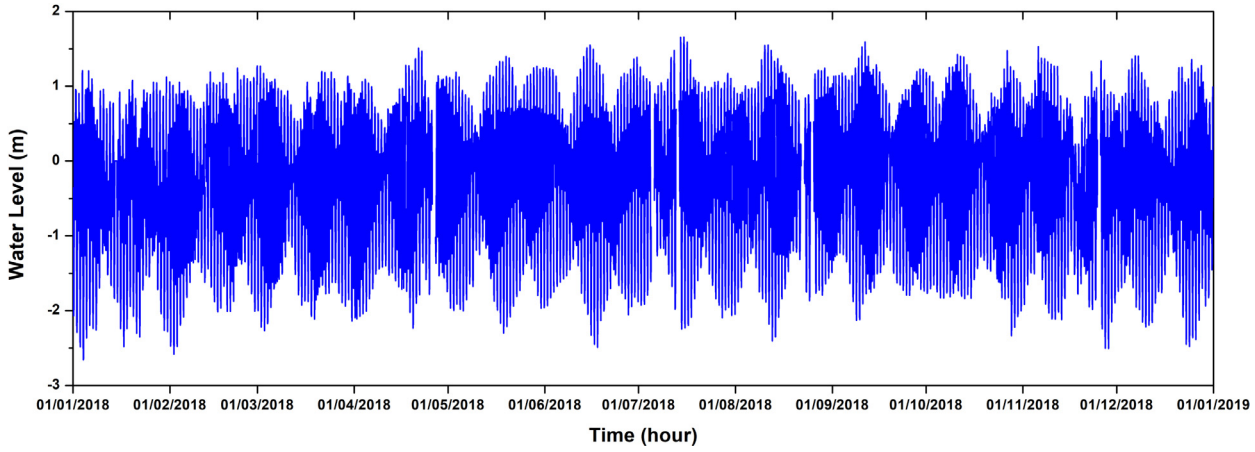

Figure 2 Time series of the hourly water level during 2018 at the entrance of Khor Abdullah.

to the mean sea level. All water level measurements are rectified to the local vertical datum known as Faw 1979 datum, the local datum in this region. The interval in water level records was one hour for the entire year of 2018.

The currents (speed and direction) measurements are carried out using a moored ADCP. The ADCP measured the water currents profile with 0.5 m space step along the water column, with a time interval of 10 minutes. However, due to the shallow nature of the study area (depth of 10 m), no remarkable changes in the water currents patterns along the water column were observed; hence, only the near-surface velocity measurements will be analyzed and discussed.

3. Results and discussion

3.1. Water level variability

Water level records in the studied area showed remarkable variations ranging from hourly to annual fluctuations. The sea-level records showed a maximum annual tidal range of about 4.32 m, from 1.66 to −2.66 m (Figure 2). This tidal range is the highest range recorded in the entire Arabian Gulf water. A similar range is observed in Kuwait bay, a semi-enclosed bay near the studied area, as indicated by Alosairi et al., 2018. Generally, the maximum tidal ranges are recorded during the spring tide, while during the neap tide, the tidal range rarely exceeds 2.5 m (Figure 2).

Table 1 displays the maximum and minimum water height during the months of 2018. The table shows that the water level reaches its highest values during the summer months, i.e., June to September. However, this behavior has been observed previously in several areas in the Arabian Gulf. It is generally attributed to the impact of the meteorological forces, particularly the atmospheric pressure, which reaches its lowest levels during the summer months (Afshar-Kaveh et al., 2020; Sultan et al., 2000). In contrast, during the winter, when the atmospheric pressure is at its highest levels, and due to the inverse relationship between this meteorological element and the sea surface, the water height is generally at the lowest level, as shown in Figure 2.

The water level variations in the study area are mainly associated with the astronomical tidal phenomenon. The harmonic analysis results of the water level in the northwest tip of the Arabian Gulf demonstrated that the astronomical tide is responsible for about 90% to 96% of water level variation (Alosairi et al., 2018; Lafta, 2021). Meanwhile, the rest of the water level variations are known as the residual water level, mainly attributed to other factors, particularly atmospherical forces. Consequently, water circulation in these regions is generally governed by tidal effects.

Table 1 Statistics of water level in the Enterence of Khor Abdullah in 2018.

Month	Minimum	Maximum
January	−2.66	1.20
February	−2.58	1.27
March	−2.27	1.26
April	−2.23	1.51
May	−2.30	1.48
June	−2.49	1.55
July	−2.24	1.66
August	−2.40	1.55
September	−2.12	1.59
October	−2.33	1.47
November	−2.50	1.53
December	−2.47	1.40

3.2. Current variability from moored measurements

The time series of near-surface currents' velocities are presented in Figure 3. However, the most common maxima exceeded 1 m/s during both the ebb and flood phases of the tidal cycle. The results illustrated that the maximum tidal current velocity generally occurs during the ebb tide. The highest flow of currents recorded during the study period reaches 1.65 m/s during the ebb tide. The monthly averages of tidal current velocities showed that the average monthly ebb velocities were also greater than the average monthly flood velocities. However, the monthly averaged flood velocities ranged between 0.56 and 0.62 m/s, while

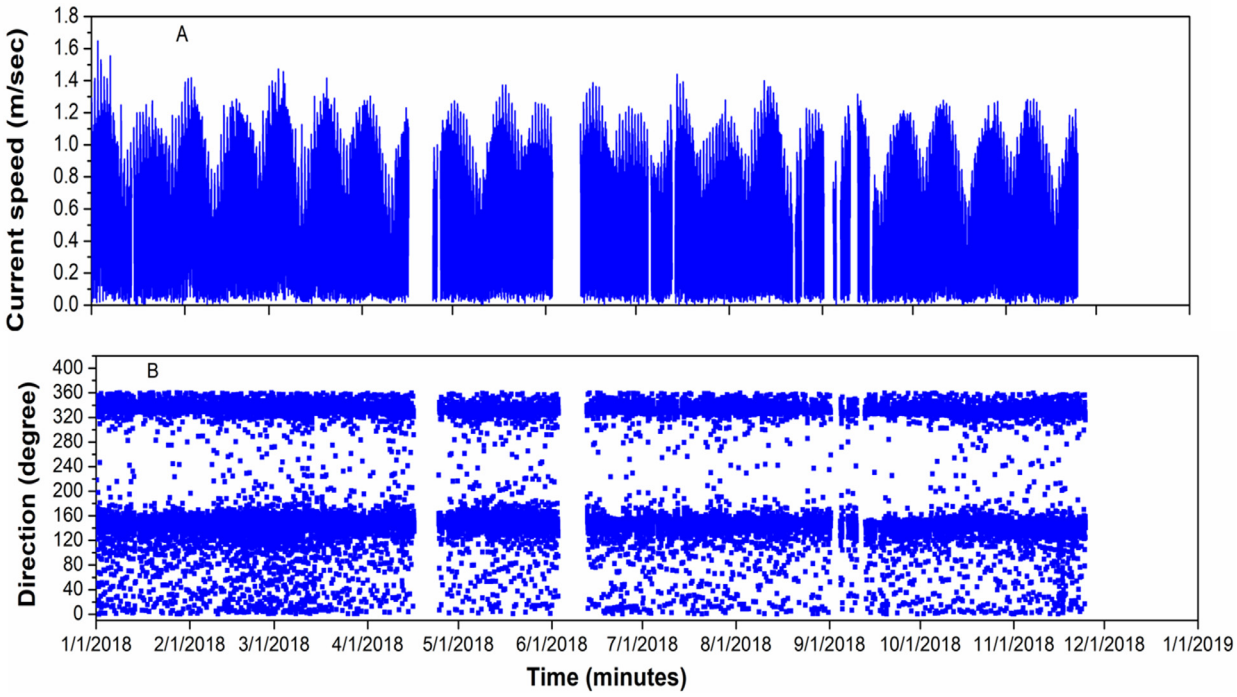

Figure 3 Time series of the currents speed (A) and direction (B) during 2018 at the entrance of Khor Abdullah.

Table 2 The ebb and flood currents statistical characteristics.

Month	Flood		Ebb	
	Mean	Maximum	Mean	Maximum
Jan.	0.62	1.27	0.69	1.65
Feb.	0.59	1.28	0.70	1.42
Mar.	0.59	1.24	0.72	1.47
Apr.	0.57	1.23	0.67	1.30
May	0.58	1.22	0.68	1.37
Jun.	0.61	1.21	0.71	1.39
Jul.	0.56	1.23	0.65	1.44
Aug.	0.58	1.36	0.68	1.40
Sep.	0.58	1.24	0.66	1.31
Oct.	0.59	1.24	0.65	1.28
Nov.	0.56	1.20	0.62	1.28

the monthly averaged ebb velocities ranged between 0.62 and 0.72 m/s (Table 2).

Based on the orientation of the study area, tidal currents have two distinguished directions, southeast during ebb tide and northwest to west-northwest through the flood tide. Other directions for the tidal current were found, but they were all very weak velocities and generally occurred during the transition period from flood tide to ebb tide and vice versa (Figure 4), and similar results were observed by Al-Hasem (2018).

Figure 5 illustrates the percentage of occurrence of various current velocity classes. The figure also shows that the flood is slightly higher for lower velocity classes, i.e., less than 0.6 m/s; meanwhile, the ebb exceeds the flood for higher velocity classes. The distribution of ebb currents demonstrated that the most frequent class of velocities is the 0.8—1 m/s group with a frequency exceeding 20%. The second significant class of ebb velocities was the 0.6—0.8 m/s group, with a frequency reaching 19.5%, followed by the class 0.4—0.6 m/s group, with a frequency of 16%. The velocity classes of 0.2—0.4 and 1—1.2 m/s seem to have an equal frequency of occurrence at about 15%. Additionally, the highest velocities of tidal currents are more frequent during the ebb phase of the tidal cycle, particularly velocities that are higher than 1.2 m/s, compared to flood currents that seem to rarely exceed 1.3 m/sec. Correspondingly, the most frequent velocity class for the flood current is the 0.8—1 m/s group, followed by 0.6—0.8 m/s and 0.4—0.6 m/s, respectively.

3.3. Harmonic analysis of currents

The characteristics of the tidal currents are investigated using the harmonic model for currents velocity recorded in the study station (Figure 1), which was performed by the World Currents package, a MATLAB application for the harmonic analysis and prediction of tides and currents (Boon, 2013). The U and V current plot in Figure 6 shows how the Khor Abdullah entrance data are distributed. Each red dot in the diagram represents the tip of a current vector with speed and direction from the origin plotted on a grid with orthogonal U and V axes. By the rotation of the U and V to the orthogonal axes U_p and V_p, the origin is first shifted to the bivariate mean position, and both axes are then rotated 59° clockwise about this point. Thus, a point lying on the U axis would have a current heading of 90°, while a point on the Up axis would have a heading of 149°.

However, Figure 6 shows that the data are arrayed from one end of the U_p axis to the other, and hence, the current

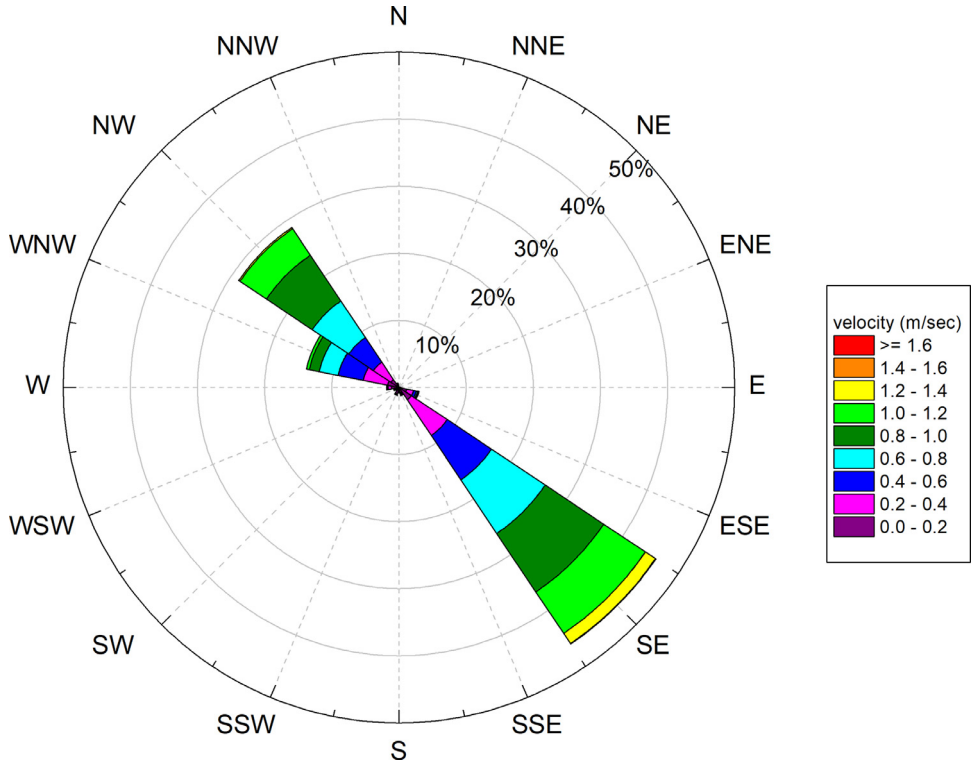

Figure 4 The rose diagram of currents at the entrance of Khor Abdullah during 2018. Up axis would have a heading of 149°.

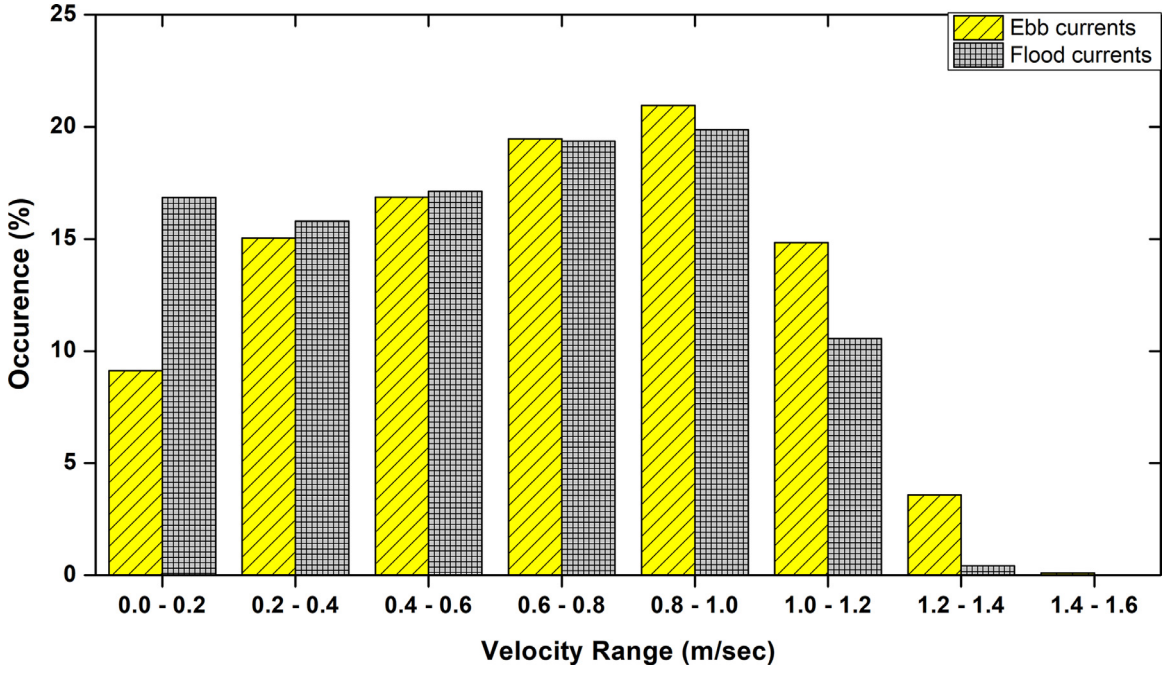

Figure 5 Percentage of various velocity classes for flood and ebb currents in Khor Abdullah Entrance.

readings projected onto this axis show an obvious spread. The U_p axis (329°—149° with respect to true north) shows the greatest spread, the maximum variance possible for any axis orientation; therefore, U_p becomes the principal axis. Meanwhile, V_p clearly has the least spread in projected values and becomes the minor axis. Moreover, the Principal Axis Variance (PAV) in Figure 6 is 0.994. The small remaining fraction of variance associated with the minor axis (0.006) suggests that not much will be missed if V_p is ignored and only U_p is considered. Thus, the currents analysis is conducted for the principle axis U_p. The harmonic analysis results of a tidal stream (Table 3) showed that the 35 astronomical constituents used by the World Currents package can explain about 98% of the total variance of the current

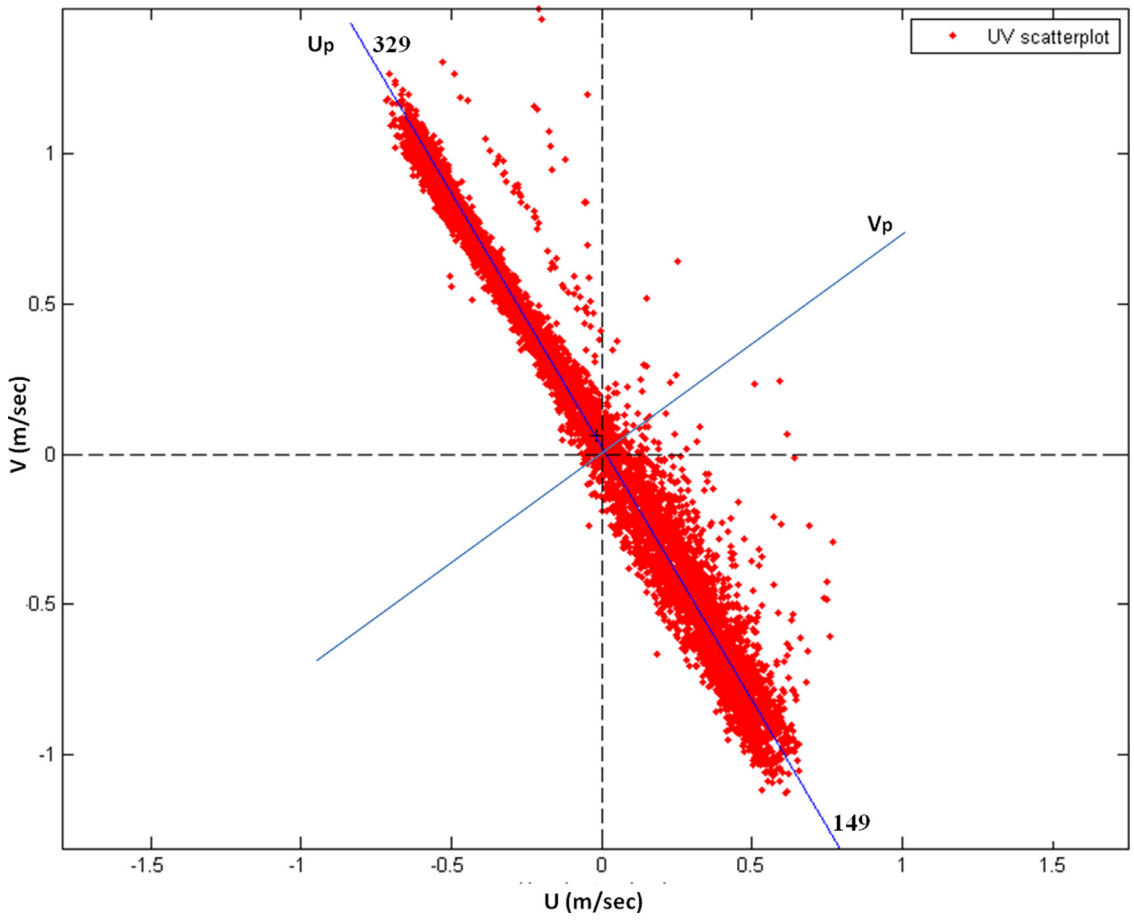

Figure 6 U,V plot of surface current readings at Khor Abdullah entrance, 2018. Principal Axis Variance (PAV) is 0.994. The flood direction is 329°; the ebb direction is 149°.

Table 3 Amplitudes (m/s) and phases (degree) for the constituents that are used in the harmonic analysis of currents in the Khor Abdullah Entrance.

Constituent	Amplitude	Phase	Constituent	Amplitude	Phase	Constituent	Amplitude	Phase
Q1	0.016	201.13	N2	0.143	263.05	MK3	0.036	275.77
RHO1	0.001	295.87	NU2	0.041	7.99	MN4	0.017	44.62
O1	0.104	305.87	M2	0.742	16.29	M4	0.047	156.99
M1	0.004	28.83	LAM2	0.027	173.17	MS4	0.036	284.15
P1	0.052	41.61	L2	0.043	25.43	S4	0.004	93.09
S1	0.009	334.91	T2	0.016	133.18	2MN6	0.012	184.26
K1	0.178	30.3	S2	0.251	138.92	M6	0.019	300.28
J1	0.01	176.14	R2	0.002	176.39	2MS6	0.022	56.44
OO1	0.006	0.23	K2	0.08	287.1	S6	0.001	67.46
MNS2	0.011	278.77	2SM2	0.018	44.33	M8	0.005	63.67
2N2	0.022	137.28	2MK3	0.048	169.95	3MS8	0.007	176.8
MU2	0.048	45.73	M3	0.004	29.16			

in the studied area during the study period. The main constituents (K_1, O_1, M_2, S_2, N_2) contributed to about 70% of this variation. The principle semidiurnal lunar constituent M_2 was the main contributor to the total variation of tidal current by about 36%, followed by S_2, K_1, N_2, and O_1. Additionally, the diurnal constituent P_1 seems to have an essential contribution to tidal currents variability in the studied area, which is in line with the findings of Pous et al. (2012), who pointed out that this constituent has an important contribution to tidal hydrodynamics of the Arabian Gulf. Correspondingly, most of the shallow water constituents seem to significantly contribute to tidal currents variation, par-

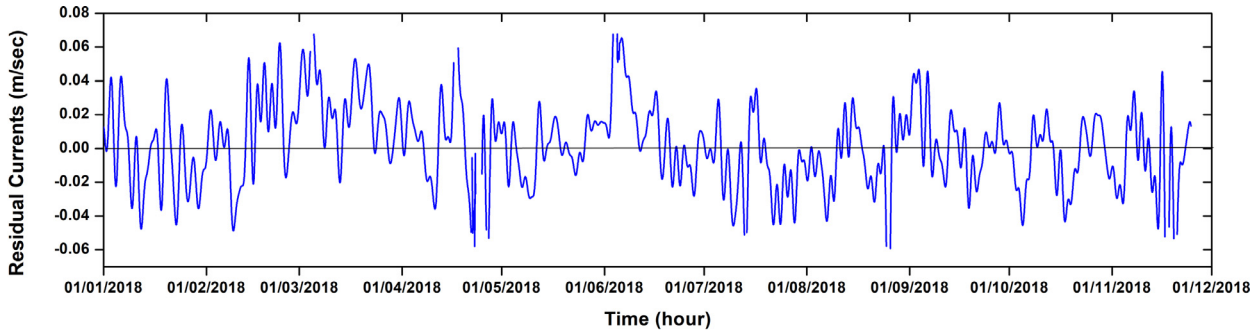

Figure 7 Residual currents in the Khor Abdullah entrance (positive values refer to the currents towards the southeast while negative values refer to the northwest direction).

ticularly $2MK_3$, M_3, MK_3, MN_4, M_4, and MS_4. However, this is not a surprising result since the studied area is a shallow coastal region with a maximum depth not exceeding 20 m (Lafta, 2021).

The form number $((O_1 + K_1)/(M_2 + S_2))$ was 0.28. Based on the classification of (Defant, 1961), the study area displays a mixed, predominantly semidiurnal tide, which is in line with the previous finding of Alosairi et al., 2018 and Lafta et al. (2020).

3.4. Residual currents

The residual currents in the studied area were obtained by applying a low-pass filter to the resulting hourly residual curve from harmonic analysis to remove all signals in semidiurnal and diurnal tidal frequencies. The cutoff frequency was 57×10^{-7} Hz (equivalent to 0.5 cycles per day). The residual currents show a seasonal fluctuation with a maximum ebb value reaching 0.0677 m/s during June and a minimum value of 0.023 m/s during October. Meanwhile, the maximum flood value of 0.058 m/s during April and a minimum of 0.02943 m/s during May (Figure 7). The direction of the residual currents shows a monthly variation. It fluctuates between northwest during five months of the study interval, i.e., January, July, August, October, and November, and southeast direction during the rest months. These fluctuations in residual direction could be attributed to the dominant wind regime in the study area, which has been well documented as ranging from northwest to southeast winds (Al Senafi and Anis, 2015; Lafta and Al-Fartusi, 2022). However, when the monthly average residual current is compared to the monthly average of the along-wind component, there appears to be no obvious relationship between them, with a correlation coefficient of less than 0.2. Hence, the origin of residual currents could belong to other forces rather than the wind force. The most probable driver could be the rivers flow since the area is known as the most estuarine part in the northwest of the Arabian Gulf. The southeast direction of residual current seems to correlate well with the river discharge during the wet months, which occur through the spring and winter months. Unfortunately, no data on river discharge is available during the study period. So, when such data is available, one can examine this hypothesis and obtain a deep understanding of the behavior of residual currents in this region.

4. Conclusion

In this study, the general behavior of tidal currents was highlighted at the entrance of Khor Abdullah in Iraq marine water at the northern tip of the Arabian Gulf. The study is based on the realistic measurements of water currents and for a relatively long period, which was never conducted previously in this region. The results illustrated that the studied area is characterized by strong tidal currents that exceed 1 m/s during both the ebb and flood phases of the tidal cycle. Additionally, the results show that the ebb velocities were generally higher than the flood velocities. The distribution of ebb and flood currents demonstrated that the most frequent class of velocities is the 0.8—1 m/s group. The results showed that the strong currents, i.e., with velocities greater than 1.5 m/s, seldom occur during flood tide and mostly occur during the ebb tide.

The harmonic analysis result demonstrated that about 98% of water currents variation was explained using 35 tidal constituents, with the remaining percentage explained using residual currents. The astronomical constituent M_2 was the main contributor to the total variation of tidal current, followed by S_2, K_1, N_2, and O_1. These five constituents account for approximately 70% of the total variance of currents in the studied area, with the remaining 30% due to the other 30 constituents. It should be noted that these findings were the primary findings and focused on the general behavior of tidal currents in this important region of the northwestern Arabian Gulf.

Acknowledgments

The author is grateful to General Company of Iraq Ports and General Acoustics company, Germany, especially Eng. Jörg Stuczynski for providing the data.

References

Afshar-Kaveh, N., Nazarali, M., Pattiaratchi, C., 2020. Relationship between the Persian Gulf sea-level fluctuations and meteorological forcing. J. Mar. Sci. Eng. 8, 285. https://doi.org/10.3390/jmse8040285

Al Senafi, F., Anis, A., 2015. Shamals and climate variability in the northern Arabian/Persian Gulf from 1973 to 2012. Int. J. Climatol. 35, 4509—4528. https://doi.org/10.1002/joc.4302
Al-hasem, A.M., 2018. Tidal Current Behaviors and Remarkable Bathymetric Change in the South-Western Part of Khor Abdullah. Kuwait. Int. J. Mar. Env. Sci. 12 (2), 118—125.
Al-Mahdi, A.A., Abdullahh, S.S., Husain, N.A., 2009. Some Features of the Physical Oceanography in Iraqi Marine Water. Mesopot. J. Mar. Sci. 24, 13—24.
Al-Mahdi, A.A., Mahmood, A.B., 2010. Some Features of Tidal Currents in Khor Abdullah. North West Arabian Gulf. J. KAU: Mar. Sci. 21 (1), 162—182.
Alosairi, Y., Imberger, J., Falconer, R.A., 2011. Mixing and flushing in the Persian Gulf (Arabian Gulf). J. Geophys. Res. 116, C03029. https://doi.org/10.1029/2010JC006769
Alosairi, Y., Pokavanich, T., Alsulaiman, N., 2018. Three-dimensional hydrodynamic modeling study of reverse estuarine circulation: Kuwait Bay. Mar. Pollut. Bull. 127, 82—96. https://doi.org/10.1016/j.marpolbul.2017.11.049
Alothman, A., Ayhan, M., 2010. Detection of Sea Level Rise within the Arabian Gulf Using Space Based GNSS Measurements and In situ Tide Gauge data. 38th COSPAR Scientific Assembly 38, 3—7.
Antoranz, A.M., Pelegri, J.L., Masciángoli, P., 2001. Tidal currents and mixing in the Lake Maracaibo estuarine system. Sci. Mar. 65 (Suppl. 1), 155—166. https://doi.org/10.3989/scimar.2001.65s1155
Bi, C., Bao, X., Ding, Y., 2019. Observed characteristics of tidal currents and mean flow in the northern Yellow Sea. J. Ocean. Limnol. 37, 461—473. https://doi.org/10.1007/s00343-019-8026-z
Boon, J.D., 2013. Secrets of the Tide: Tide and Tidal Current Analysis and Predictions, Storm Surges and Sea Level Trends. Elsevier, 224 pp.
Chen, Y.R., Paduan, J.D., Cook, M.S., Chuang, L.Z., Chung, Y.J., 2021. Observations of Surface Currents and Tidal Variability Off of Northeastern Taiwan from Shore-Based High Frequency Radar. Remote Sens. 13, 3438. https://doi.org/10.3390/rs13173438
Defant, A., 1961. Physical Oceanography, vol. 1. Pergamon Press, London, 729.
Hoitink, A.J.F., Buschman, F.A., Vermeulen, B., 2009. Continuous measurements of discharge from a horizontal acoustic Doppler current profiler in a tidal river. Water Resour. Res. 45 (11), 1—3. https://doi.org/10.1029/2009WR007791
Jin, G., Pan, H., Zhang, Q., Lv, X., Zhao, W., Gao, Y., 2018. Determination of harmonic parameters with temporal variations: An enhanced harmonic analysis algorithm and application to internal tidal currents in the south China Sea. J. Atmos. Ocean. Tech. 35 (7), 1375—1398. https://doi.org/10.1175/jtech-d-16-0239.1
Kämpf, J., Sadrinasab, M., 2006. The circulation of the Persian Gulf: A numerical study. Ocean Sci. 2, 27—41. https://doi.org/10.5194/os-2-27-2006
Khedr, A.M., Abdelrahman, S.M., Alam El-Din, K.A., 2018. Currents and sea level variability of Alexandria Coast in Association with Wind Forcing. J. KAU: Mar. Sci. 28, 27—42. https://doi.org/10.4197/Mar.28-2.3
Kowalik, Z., Marchenko, A., Brazhnikov, D., Marchenko, N., 2015. Tidal currents in the western Svalbard Fjords. Oceanologia 57 (4), 318—332. https://doi.org/10.1016/j.oceano.2015.06.003
Lafta, A.A., 2021. Influence of atmospheric forces on sea surface fluctuations in Iraq marine water, northwest of Arabian Gulf. Arab. J. Geosci. 14, 1639. https://doi.org/10.1007/s12517-021-07874-x
Lafta, A.A., 2022. Investigation of tidal asymmetry in the Shatt Al-Arab river estuary, Northwest of Arabian Gulf. Oceanologia 64 (2), 376—386. https://doi.org/10.1016/j.oceano.2022.01.005
Lafta, A.A., Al-Fartusi, A.J., 2022. General characteristics of surface waves in Iraq marine water, Northwest of Arabian Gulf. Arab. J. Geosci. 15, 1598. https://doi.org/10.1007/s12517-022-10884-y
Lafta, A.A., Altaei, S.A., Al-Hashimi, N.H., 2020. Impacts of potential sea-level rise on tidal dynamics in Khor Abdullah and Khor Al-Zubair, northwest of Arabian Gulf. Earth Syst. Environ. 4, 93—105. https://doi.org/10.1007/s41748-020-00147-9
Madah, F., Sameer, G., 2022. Numerical Simulation of Tidal Hydrodynamics in the Arabian Gulf. Oceanologia 64 (2), 327—345. https://doi.org/10.1016/j.oceano.2022.01.002
Najafi, H.S., 1997. Modeling tides in the Persian Gulf using dynamic nesting Ph.D. thesis. Univ. Adelaide, South Australia.
Poulain, P.M., Centurioni, L., 2015. Direct measurements of World Ocean tidal currents with surface drifters. J. Geophys. Res.-Oceans 120 (10), 6986—7003. https://doi.org/10.1002/2015JC010818
Pous, S., Carton, X., Lazure, P., 2012. A Process Study of the Tidal Circulation in the Persian Gulf. Open J. Mar. Sci. 02 (04), 131—140. https://doi.org/10.4236/ojms.2012.24016
Ranjbar, M.H., Etemad-Shahidi, A., Kamranzad, B., 2020. Modeling the combined impact of climate change and sea-level rise on general circulation and residence time in a semi-enclosed sea. Sci. Total Environ. 740, 140073. https://doi.org/10.1016/j.scitotenv.2020.140073
Reynolds, R.M., 1993. Physical oceanography of the Gulf, Strait of Hormuz, and the Gulf of Oman: results from the Mt Mitchell expedition. Mar. Pollut. Bull. 27, 35—59. https://doi.org/10.1016/0025-326X(93)90007-7
Sadrinasab, M., Kämpf, J., 2004. Three-dimensional flushing times of the Persian Gulf. Geophys. Res. Lett. 31, 1—4. https://doi.org/10.1029/2004GL020425
Shin, H.R., Lee, J.H., Kim, C.H., Yoon, J.H., Hirose, N., Takikawa, T., Cho, K., 2022. Long-term variation in volume transport of the Tsushima warm current estimated from ADCP current measurement and sea level differences in the Korea/Tsushima Strait. J. Marine Syst. 232. https://doi.org/10.1016/j.jmarsys.2022.103750
Siddig, N.A., Al-Subhi, A.M., Alsaafani, M.A., 2019. Tide and mean sea level trend in the west coast of the Arabian Gulf from tide gauges and multi-missions satellite altimeter. Oceanologia 61 (4), 401—411. https://doi.org/10.1016/j.oceano.2019.05.003
Sterl, M.F., Delandmeter, P., van Sebille, E., 2020. Influence of barotropic tidal currents on transport and accumulation of floating microplastics in the global open ocean. J. Geophys. Res.-Oceans 125, e2019JC015583. https://doi.org/10.1029/2019JC015583
Sultan, S.A., Moamar, M.O., Elghribi, N.M., Williams, R., 2000. Sea level changes along the Suadi coast of the Arabian Gulf. Indian J. Geo-Mar Sci. 29, 191—200. http://nopr.niscair.res.in/handle/123456789/25532
Truong, D.D., Tri, D.Q., Don, N.C., 2021. The impact of waves and tidal currents on the sediment transport at the sea port. Civil Eng. J. 7 (10), 1634—1649.
Zakaria, S., Al-Ansari, N., Knutsson, S., 2013. Historical and future climatic change scenarios for temperature and rainfall for Iraq. J. Civ. Eng. Archit. 7, 1574—1594. https://doi.org/10.17265/1934-7359/2013.12.012